Theoretical investigation of the vibrational properties of BeH_2 and Li_2BeH_4

H. Iddir,[1] P. Zapol,[1] and A. I. Kolesnikov[2]
[1]*Materials Science Division, Argonne National Laboratory, Argonne, Illinois 60439, USA*
[2]*Spallation Neutron Source, Oak Ridge National Laboratory, Oak Ridge, Tennessee 37831, USA*
(Received 23 February 2009; revised manuscript received 5 June 2009; published 14 October 2009)

First-principles calculations of BeH_2 and Li_2BeH_4 were performed and compared to inelastic neutron scattering. The crystal structure ($P2_1/c$ space group) of Li_2BeH_4 contains BeH_4 tetrahedral units similar to those in α-BeH_2 (*Ibam* space group) but separated from each other by Li atoms. Calculated vibrational density of states revealed the origin of the observed major vibrational modes. Charge-density maps and electronic density of states indicate interplay between covalent and ionic bondings in Li_2BeH_4 and provide a better understanding of the nature of the bonding in these materials.

DOI: 10.1103/PhysRevB.80.134111 PACS number(s): 61.50.−f, 63.20.dk, 71.15.Mb, 61.05.fg

I. INTRODUCTION

Beryllium hydride, BeH_2, exhibits one of the highest hydrogen-to-metal mass ratios (more than 18 wt. %) and presents fundamental and technological interest as a potential material for energy-conversion devices, rocket propellant, nuclear industry, and hydrogen storage. To release hydrogen, the BeH_2 should be heated to above 250 °C. Doping with other light elements, e.g., Li, to keep the compound's weight low, could be a possible way to decrease the hydride decomposition temperature to a practically acceptable value. Li-complex hydrides, such as $LiBH_4$ (Refs. 1 and 2) and $LiNH_2$,[3] have attracted interest as potential hydrogen storage materials. An understanding of doping effect on the beryllium-hydrogen interaction is a logical way to investigate and design prospective hydrogen storage materials.

The typically synthesized solid beryllium hydride BeH_2 has an amorphous structure,[4] which can be transformed to crystalline phases under high pressure and temperature.[5] The α-BeH_2 is the lowest-pressure crystalline phase, which has a body-centered orthorhombic structure. Both these hydrides, amorphous, and crystalline contain similar building blocks: corner-shared tetrahedral units of BeH_4, with similar interatomic distances. It is commonly assumed that Be and H atoms are connected by a covalent bond.[6,7] Although BeH_2 has been discovered about half a century ago, its vibrational dynamics in solid state has not been fully investigated up to now. There is only a limited information on infrared (IR) spectra of amorphous BeH_2 (Ref. 4); other literature IR data were related either to free linear BeH_2 molecules[8] or to BeH_2 molecules or one-dimensional $(BeH_2)n$ polymer chains in matrix (argon, neon, hydrogen).

Inelastic neutron scattering (INS) is the most effective experimental method to study dynamics of hydrogen-containing materials because of its anomalously high sensitivity to hydrogen atoms and the straightforward comparison with the computational results. As was shown in numerous previous INS investigations of metal hydrides, the high sensitivity of the vibrational density of states (VDOS) to the structural changes often revealed valuable insights into the hydrogen potential and the strength of the Me-H interaction, often not accessible by other techniques. Recent INS experiments[9] were carried out on HRMECS (for BeH_2) and LRMECS (for Li_2BeH_4) spectrometers installed at Intense Pulsed Neutron Source in Argonne National Laboratory.[10] The collected data were reduced to dynamical structure factor, $S(Q,E)$, which was then transferred to generalized vibrational density of states, $G(E)$, according to the following expression:

$$G(E) = S(Q,E)\frac{2mE}{\hbar^2 Q^2[n(E,T)+1]}, \quad (1)$$

where Q and E are the neutron momentum and energy transfers, m is atomic unit mass, and $n(E,T)=1/[\exp(E/k_BT)-1]$ is a population Bose factor. Figure 1 shows the obtained $G(E)$ spectra. The spectrum for BeH_2 sample (curve 1) consists of three broad vibrational bands between 50–115 meV (with maximum at $E_{max}\approx 97$ meV), 115–190 meV (with $E_{max}\approx 162$ meV), and 190–260 meV (with $E_{max}=224$ meV). Based on the assignments in IR study[4] these bands, respectively, can be attributed to bending (ν_2), symmetrical (ν_1), and antisymmetrical (ν_3) stretching modes of Be-H bonds. The spectrum for Li_2BeH_4 clearly shows a strong softening by about 20–30 meV of all vibrational bands, which in addition become split. The strong shift to lower energy of the bending modes (ν_2) was initially ascribed to a weaker ionic-type Li-H interaction compared to the covalent one for Be-H bond.[9] This would explain why in Li_2BeH_4 the bending modes of terminal Be-H bond in "isolated" BeH_4 tetrahedra appeared at much lower energies compared to the similar modes in continuous network of corner-shared tetrahedra in BeH_2 sample. The observed differences in the Be-H stretching modes should correspond to about 20–70 % decrease in the strength of the Be-H covalent bonds in Li_2BeH_4 compared to BeH_2: $(224/204)^2\approx 1.2$ and $(162/123)^2\approx 1.7$, where 224, 204, 162, and 123 are the energy positions of the corresponding peaks. Therefore we can expect that the mobility of hydrogen atoms in Li-doped BeH_2 should be higher due to weaker Be-H interaction. This should also lead to lower dissociation temperature, a very important property for hydrogen storage materials. First-principles calculations can further validate these considerations and clarify the assignments of vibrational modes.

Phonon spectra of the crystalline α-BeH_2 were investigated theoretically,[11,12] but no such study was done for Li-

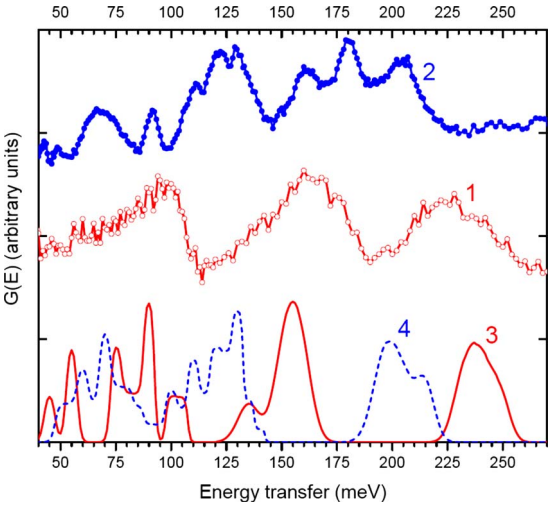

FIG. 1. (Color online) Vibrational spectra of BeH_2 (1–experimental, 3–theoretical) and Li_2BeH_4 (2–experimental, 4–theoretical).

doped Be hydride. The structure of amorphous Li_2BeH_4 is not yet solved completely, but one can assume that its short-range order is similar to that in the crystalline phase. The crystal structure of Li_2BeH_4 (Ref. 13) contains BeH_4 tetrahedral units similar to those in BeH_2, but these tetrahedra are separated from each other by Li atoms and are not corner-shared any more, as in BeH_2. Here we present a first-principles study of BeH_2 and Li_2BeH_4, focusing on effect of Li doping on the strength of Be-H interaction, and compare the results with recent experimental data[9] on amorphous samples.

II. COMPUTATIONAL DETAILS

To understand the microscopic mechanism of hydrogen interaction with Be and the effect of Li doping on vibrational spectra we carried out first-principles calculations. The calculations were performed using density-functional theory with plane-wave basis sets and Perdew-Wang 91 exchange-correlation functional as implemented in the Vienna *ab initio* simulations package (VASP).[14] We have used the projector augmented wave (PAW) potentials with cutoffs of 400 and 450 eV, respectively, for BeH_2 and Li_2BeH_4. The atomic positions were relaxed until the Hellmann-Feynman forces were less than 4×10^{-3}, and 10^{-5} eV/Å, respectively. Brillouin zone integrations were performed using Monkhorst-Pack k-points grids of up to $11\times11\times11$. The crystal structure of body-centered orthorhombic α-BeH_2, *Ibam* space group, as determined in Ref. 5, was optimized using 18 atom unit cell. The calculated lattice parameters (a=8.89 Å, b=4.08 Å, and c=7.59 Å) are in a good agreement with experiment (a=9.082 Å, b=4.16 Å, and c=7.707 Å). Our results are also in good agreement with a recent theoretical study[12] (a=8.95 Å, b=4.12 Å, and c=7.63 Å).

For Li_2BeH_4, we have used the structure of Li_2BeD_4 ($P2_1/c$ space group, a=7.0623 Å, b=8.3378 Å, c=8.3465 Å, and β=93.58°) determined by Bulychev *et al.*[13] and optimized internal coordinates only. The above-mentioned α-Li_2BeH_4 structure was also shown to be the stable phase in a recent theoretical study.[15] The crystal phonon frequencies for hydrogen were calculated using numerical differences with 18-atom cell for BeH_2 and 56-atom cell for Li_2BeH_4. All the atomic coordinates of H were varied, with finite displacements of 0.02 Å. To verify the approximations, the vibrational frequencies of H in BeH_2 for 0.01 and 0.03 Å displacements were also calculated; the shift in the frequencies was less than 1 meV.

The INS spectra of BeH_2 and Li_2BeH_4 mostly originate from neutron scattering on hydrogen atoms. The contributions from metal atoms are small as the total neutron-scattering cross section of H is about 11 and 60 times larger than that of Be and Li, respectively.[16] Furthermore, in the case of optical vibrations the scattering intensity is inversely proportional to the atomic mass, which gives additional nine and seven times stronger signal for H compared to that for Be and Li, therefore the INS spectra of BeH_2 and Li_2BeH_4 well represent the density of states of optical H vibrations. Therefore, heavy atoms were held fixed in our calculations, resulting in 36 normal modes for BeH_2 and 96 normal modes for Li_2BeH_4. The calculated vibrational densities of states in Fig. 1 were convoluted with spectrometer resolution function, which allowed direct comparison with the experimental data.[9] Vibrational eigenstates were used to identify the modes, and typical atomic displacements in different bands of the spectra are shown in Fig. 2.

III. RESULTS AND DISCUSSION

A. Vibrational properties

Our calculated VDOS for BeH_2 consists of three bands at 220–260 meV, 120–170 meV, and below 110 meV. These bands are identified in experiments as antisymmetric stretch, symmetric stretch, and bending modes. Previous first-principles calculations[12] (without fixed heavy atoms) have obtained very similar results, i.e., the VDOS exhibit three bands with energies about 230–260 meV, 130–175 meV, and below 105 meV. Comparison of the calculated [Fig. 2(a)] and experimental (curves 1 and 3 in Fig. 1) $G(E)$ spectra shows an overall good qualitative agreement. The calculated antisymmetric (ν_3) and symmetric (ν_1) stretching Be-H modes in BeH_2 appeared, respectively, at slightly higher and lower energies compared to the experimental data. The calculated band for symmetric stretching modes consists of a strong peak and a weak one at lower energy, which corresponds to the low-energy shoulder in the experimental spectrum. Note that the stretching modes in BeH_2 also involve some bending as the corresponding displacement vectors are not aligned along the Be-H bonds in the corner shared tetrahedral network. Symmetric and antisymmetric stretchings refer to the displacement symmetry of a single H atom between two Be atoms. Among all the calculated vibrational modes in BeH_2, the symmetric stretching mode gives rise to the largest shape deformations in the BeH_4 tetrahedral units, which is consistent with the largest Raman intensities of these modes.[9] The antisymmetric modes give rise to the largest Be-H bond length change and hence larger infrared signal, consistent with the recent observations of Sampath *et al.*[9] The calcu-

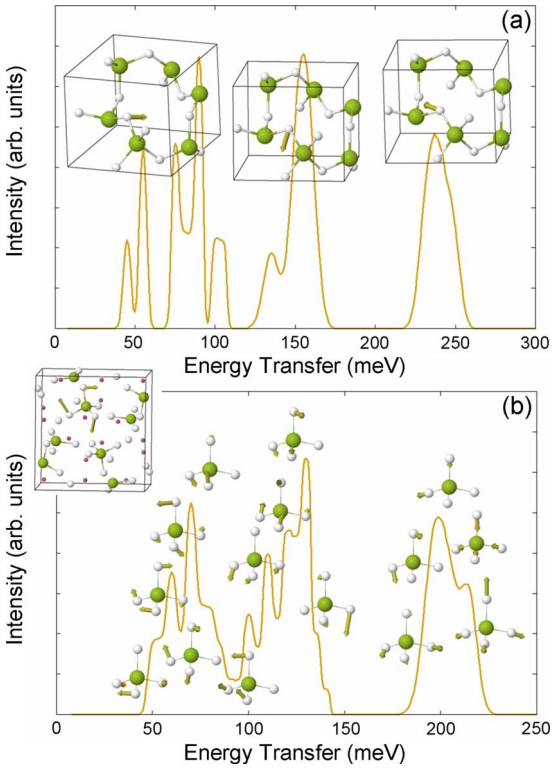

FIG. 2. (Color online) Calculated phonon density of states for the: (a) orthorhombic α-BeH_2. Selected phonon eigenvectors shown with arrows represent the three major regions of the spectrum: antisymmetric stretching, symmetric stretching, and bending modes, in the order of decreasing frequencies. H and Be atoms are shown as medium white and large green spheres, respectively. (b) Monoclinic Li_2BeH_4. Selected phonon eigenvectors, each shown in a single tetrahedron with arrows, exhibit the three major regions of the spectrum. The highest region includes both symmetric and antisymmetric stretching unlike the two separate peaks in BeH_2; the two lower regions represent bending and bending-twisting-rocking modes, respectively. Top left, the unit cell used for the calculations. Li atoms are shown as small purple spheres.

lated band of bending modes appeared in the same energy range as in the experimental spectrum but more structured since calculations were performed for a perfect crystal.

The calculated $G(E)$ spectrum for Li_2BeH_4 shows lower frequencies of the stretching and bending Be-H modes compared to BeH_2, in good agreement with the experiment. Contrary to the BeH_2 case, in Li_2BeH_4 the stretching modes are true stretching modes as the displacement vector in this case is aligned with the Be-H bond. Also, the symmetry assignment now refers to a single Be atom with four H atoms (corners of the tetrahedra) vibrating in either symmetric (expansion or contraction of the tetrahedra breathing modes) or antisymmetric (deformation of the tetrahedra) modes. The near degeneracy of symmetric and antisymmetric stretch modes, which is evident in separated BeH_4 tetrahedra of Li_2BeH_4 shown in Fig. 2(b), is removed by the corner sharing of tetrahedra in BeH_2. Sharing of each hydrogen atom by two Be in BeH_2 increases its binding energies and, consequently, its stretching frequency. As noted above, a stretch mode in BeH_2 is not a pure stretch since a displacement

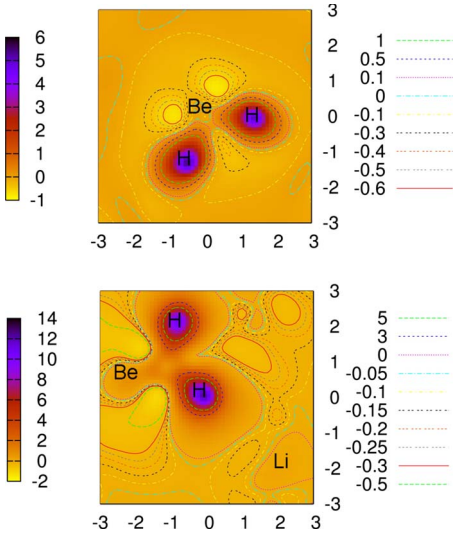

FIG. 3. (Color online) Charge-density-difference contour plots: $10^{-4}(10^{-5}) \times e/(\text{a.u.})^3$ for (bottom) Be-H-Li plane in Li_2BeH_4 and for (top) H-Be-H plane in BeH_2

vector is a sum of corresponding displacement vectors for two Be-H bonds sharing the same H atom. This results in change in angles within corner-sharing BeH_4 tetrahedra, which is attributed to bending modes in isolated BeH_4 tetrahedra. Therefore, Li doping results in separation of the tetrahedra and shifts the symmetric and antisymmetric stretch frequencies to the single split peak, while the rocking and twisting modes come apart from the peak of bending modes as shown in Fig. 2(b).

This explains the experimental observation in the shift of the stretching modes in Li_2BeH_4 interpreted as their softening. This appeared to be surprising because Li-H interaction is weaker than Be-H interaction and, thus, one would expect stronger Be-H covalent bond and a shift of the corresponding stretching modes to higher frequencies. This tendency is usually observed in molecular crystals with hydrogen bonds: decrease in the hydrogen bond strength between the molecules results in increase in the corresponding intramolecular stretching modes, e.g., see different ice phases.[17] Thus, the obtained results suggest strong decrease in Be-H interaction in the presence of Li atoms due to reduction in the number of the Be-H bonds from two per H atom to one, although a stronger one, providing a full explanation of the experimental results.

B. Electronic properties

To better understand the electronic effect of Li doping on the Be-H bond, we have plotted in Fig. 3 charge-density-difference contour maps for the hydrides. The electron density difference for BeH_2 clearly shows an increase in the electronic charge around H atom, with a considerable polarization toward Be atom, which results in increased charge overlap between Be and H atoms suggesting a mixed ionic-covalent character of the bond. The isosurfaces in Figs. 4(b) and 4(d) provide more spatial detail on electron density redistribution upon formation of chemical bonds. This result is

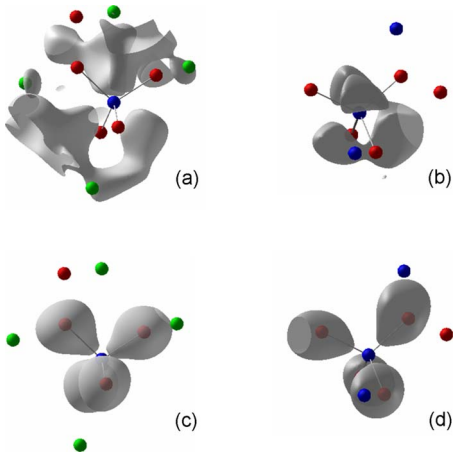

FIG. 4. (Color online) Charge density isosurfaces for Li_2BeH_4 at (a) −0.002 $e/(a.u.)^3$ and (c) +0.007 $e/(a.u.)^3$ and for BeH_2 at (b) −0.0056 $e/(a.u.)^3$ and (d) +0.007 $e/(a.u.)^3$

also consistent with the electron localization function (ELF) shown in Fig. 5, which indicates that the ELF around H is not spherical in agreement with the interpretation of ELF in covalent bonding.[18] ELF values around $\frac{1}{2}$ (homogenous electron gas) can be readily seen between the hydrogen atoms, suggesting a degree of delocalization of electrons in BeH_2. Previous calculations of BeH_2 using GGA-PBE functional interpreted an increase in the electronic density between Be and H as a purely covalent bonding.[6]

The Be-H bonding remains similar for Li_2BeH_4 as Li does not seem to considerably affect the nature of the bonding. The density difference around Be-H bonds shown in Fig. 3 and in Figs. 4(a) and 4(c) in the case of Li_2BeH_4 resembles its counterpart in BeH_2, with an overall lesser amount of charge transfer. Charge depletion around Li and along the Li-H bond is a clear signature of an ionic bonding character. The bonding characteristics in Li_2BeH_4 are somewhat similar to $KAlH_4$ investigated earlier by Vajeeston *et al.*,[19] in which $K\text{-}AlH_4$ was found to be ionic and Al-H bond to be mixed ionic-covalent with a stronger directional covalent character. In our case, however, Be-H does not exhibit the same directional behavior observed in $KAlH_4$ compound, inferring a more ionic character of the Be-H bond than Al-H bond. The charge-density-difference contours also show that the radii of H atoms have increased from a neutral atomic covalent value of 0.37 Å, consistent with the increased electron charge density around H in both compounds. The contours seem to be more spherical in Li_2BeH_4 than in BeH_2, which suggests a stronger covalent character in the latter.

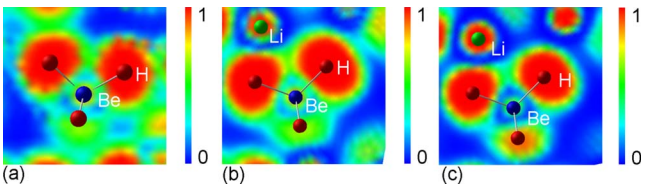

FIG. 5. (Color online) Electron localization function: (a) BeH_2 [(b) and (c)] Li_2BeH_4. (a) and (b) ELF in H-Be-H planes. (c) ELF in H-Li-H plane.

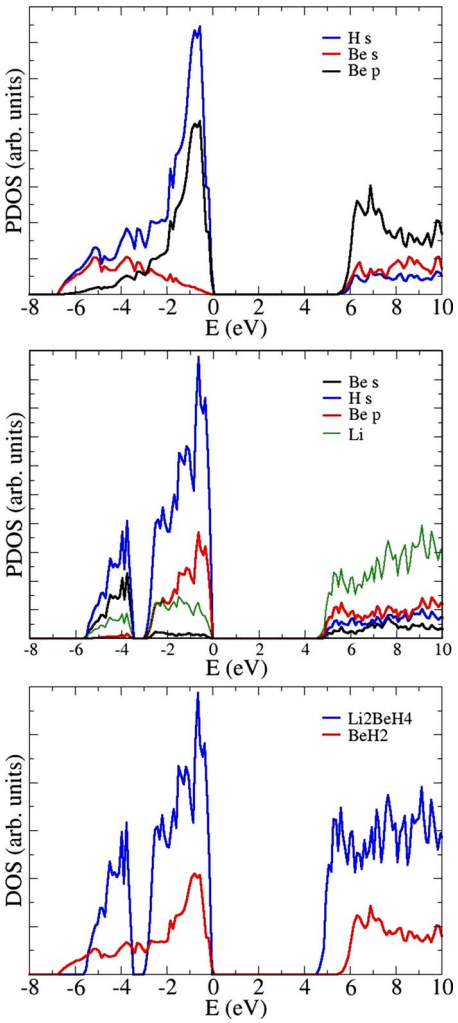

FIG. 6. (Color online) Partial density of states for (top) α-BeH_2 and (middle) Li_2BeH_4 and (bottom) total density of states for both hydrides. The zero energy is at the Fermi level.

The bonding and charge transfer obtained from the charge-density-difference maps is in agreement with Bader charge analysis. In Li_2BeH_4, the total Bader charges for Li, Be, and H atoms are 0.88, 1.27, and −0.75, respectively, and, in BeH_2, the Bader charges on Be and H are 1.34 and −0.67, respectively. The charge depletion around Be is higher in the latter case, in agreement with our density-difference maps.

The overall charge of a BeH_4 unit within Li_2BeH_4 crystal is $-1.73e$. Isolated BeH_4 tetrahedra are stabilized only in the −1 and −2 charged states since we have checked that neither an isolated neutral BeH_4 tetrahedron nor such a tetrahedron surrounded by eight Li atoms in Li_2BeH_4 crystallographic positions are stable. In the absence of crystal field, one of the H atoms of the BeH_4 breaks a bond and reacts with a Li atom, resulting in a substantial charge transfer. This indicates that even in amorphous Li_2BeH_4 some degree of ordering has to be present to account for the observed vibrational spectra. The converged geometry for an isolated BeH_4^{2-} tetrahedron is close to its configuration in the Li_2BeH_4 crystal, with larger Be-H bond lengths (1.49–1.52 Å) compared to (1.43–1.44 Å) in the presence of Li. The normal modes (12 modes) for the isolated BeH_4^{2-} also resemble the Li_2BeH_4

VDOS, with one symmetric mode at 176 meV, three antisymmetric stretching modes at 148–156 meV and bending-twisting modes at 81–94 meV. The calculated Li_2BeH_4 vibrational modes have a one-to-one correspondence with the modes of the isolated BeH_4^{2-} tetrahedral unit but at slightly higher frequencies, consistent with the decreased bond lengths and with a richer structure due to the interactions of neighboring BeH_4 units.

Previous study[7] of electronic structure of α-BeH_2 have shown that the Be-2*s* and H-1*s* states are energetically degenerate in the energy range −6.25 to 0 eV and the valence electron charge density is finite between the Be and H atoms. This corresponds very well to our calculated widths of the upper valence band formed by H and Be states (Fig. 6). However, in the presence of Li this band is split into two subbands between −5.5 and 0 eV, the lower subband is formed by both Be 2*s* and H states and the upper subband has no evidence of the spherical Be 2*s* states but rather a *p*-type contribution of the promoted Be 2*s* states to the DOS, consistent with the sp^3 hybridization of Be orbitals in the tetrahedral symmetry. This splitting indicates that the separation of BeH_4 tetrahedra in Li_2BeH_4 reduces the covalent Be-H interactions.

IV. CONCLUSIONS

In summary, we have found that Li doping of BeH_2 results in Li separating BeH_4 tetrahedra and stabilizing them through charge transfer to H without forming covalent bonds to H atoms, which drastically changes BeH_2 structure and vibrational properties. Coordination of H by a single Be atom in Li_2BeH_4 as opposed to two Be atoms in BeH_2 results in a weaker bonding and downward shift of vibrational frequencies as well as near degeneracy of symmetric and antisymmetric stretching modes of the tetrahedra. Understanding the mechanism of such bond weakening achieved by doping of metal hydrides will help design materials with tailored hydrogen binding energies.

ACKNOWLEDGMENTS

The work at Argonne National Laboratory was supported by the Office of Basic Energy Sciences, Division of Materials Sciences, (U.S.) Department of Energy under Contract No. DE-AC02-06CH11357 and the work at Spallation Neutron Source was supported by Oak Ridge National Laboratory, managed by UT-Battelle, LLC, for the (U.S.) Department of Energy under Contract No. DE-AC05-00OR22725. Use of computer resources from the DOE's Environmental Molecular Sciences Laboratory located at Pacific Northwest National Laboratory is gratefully acknowledged. We thank S. Sampath and J. L. Yarger for helpful discussions.

[1] N. Ohba, K. Miwa, M. Aoki, T. Noritake, S. I. Towata, Y. Nakamori, S. I. Orimo, and A. Züttel, Phys. Rev. B **74**, 075110 (2006).
[2] K. Miwa, N. Ohba, S. I. Towata, Y. Nakamori, and S. I. Orimo, Phys. Rev. B **69**, 245120 (2004).
[3] B. Magyari-Köpe, V. Ozoliņš, and C. Wolverton, Phys. Rev. B **73**, 220101(R) (2006); P. Chen, Z. Xiong, J. Luo, J. Lin, and K. L. Tan, Nature (London) **420**, 302 (2002).
[4] M. D. Senin, V. V. Akhachinskii, Y. E. Markushkin, N. A. Chirin, L. M. Kopytin, I. P. Mikhalenko, N. M. Ermolaev, and A. V. Zabrodin, Inorg. Mater. **29**, 1416 (1993).
[5] G. S. Smith, Q. C. Johnson, D. K. Smith, D. E. Cox, R. L. Snyder, R. S. Zhou, and A. Zalkin, Solid State Commun. **67**, 491 (1988).
[6] U. Hantsch, B. Winkler, and V. Milman, Chem. Phys. Lett. **378**, 343 (2003).
[7] P. Vajeeston, P. Ravindran, A. Kjekshus, and H. Fjellvåg, Appl. Phys. Lett. **84**, 34 (2004).
[8] P. F. Bernath, A. Shayesteh, K. Tereszchuk, and C. Reginald, Science **297**, 1323 (2002); A. Shayesteh, K. Tereszchuk, P. F. Bernath, and R. Colin, J. Chem. Phys. **118**, 1158 (2003).
[9] S. Sampath, A. I. Kolesnikov, K. M. Lantzky, and J. L. Yarger, J. Chem. Phys. **128**, 134512 (2008).
[10] C. K. Loong, S. Ikeda, and J. M. Carpenter, Nucl. Instrum. Methods Phys. Res. A **260**, 381 (1987); A. I. Kolesnikov, J. M. Zanotti, and C. K. Loong, Neutron News **15**, 19 (2004).
[11] R. Yu, P. K. Lam, and J. Head, Solid State Commun. **70**, 1043 (1989).
[12] L. G. Hector, J. F. Herbst, W. Wolf, P. Saxe, and G. Kresse, Phys. Rev. B **76**, 014121 (2007).
[13] B. M. Bulychev, R. V. Shpanchenko, E. V. Antipov, D. V. Sheptyakov, S. N. Bushmeleva, and A. M. Balagurov, Inorg. Chem. **43**, 6371 (2004).
[14] G. Kresse and J. Furthmüller, Phys. Rev. B **54**, 11169 (1996); Comput. Mater. Sci. **6**, 15 (1996).
[15] C. H. Hu, D. M. Chen, Y. M. Wang, D. S. Xu, and K. Yang, Phys. Rev. B **75**, 224108 (2007).
[16] V. F. Sears, Neutron News **3**, 26 (1992).
[17] J. C. Li, J. Chem. Phys. **105**, 6733 (1996); A. I. Kolesnikov, J. C. Li, S. F. Parker, R. S. Eccleston, and C. K. Loong, Phys. Rev. B **59**, 3569 (1999).
[18] A. Savin, A. D. Becke, J. Flad, R. Nesper, H. Preuss, and H. G. von Schnering, Angew. Chem., Int. Ed. Engl. **30**, 409 (1991).
[19] P. Vajeeston, P. Ravindran, A. Kjekshus, and H. Fjellvåg, J. Alloys Compd. **404-406**, 377 (2005).